

# Intracavity generation of radially polarized CO<sub>2</sub> laser beams based on a simple binary dielectric diffraction grating

Tobias Moser, Jürg Balmer, Danaë Delbeke, Peter Muys, Steven Verstuyft, and Roel Baets

We present experimental results on the intracavity generation of radially polarized light by incorporation of a polarization-selective mirror in a CO<sub>2</sub>-laser resonator. The selectivity is achieved with a simple binary dielectric diffraction grating etched in the backsurface of the mirror substrate. Very high polarization selectivity was achieved, and good agreement of simulation and experimental results is shown. The overall radial polarization purity of the generated laser beam was found to be higher than 90%. © 2006 Optical Society of America

OCIS codes: 050.1950, 140.3300, 140.3390, 140.3410, 140.3470, 260.5430.

## 1. Introduction

High-power CO<sub>2</sub> laser systems are predominantly linearly polarized with uniform polarization across the laser beam. In material processing applications such as cutting sheet metals, this linearly polarized laser mode is transformed extracavity to a circularly polarized laser beam to exhibit an independent direction and symmetrical performance in the material processing. The efficient generation of high-power radially polarized laser beams has gained interest in the past years due to several advantages in different fields of application. Niziev *et al.*,<sup>1</sup> for example, proposed theoretically that the use of radially polarized TEM<sub>01</sub> mode, with the direction of the electric field pointing in the radial direction, can enhance the cutting efficiency of metal up to 2 times as compared to cutting with linear polarization. Another field of interest is the acceleration of particles,<sup>2</sup> where one can make use of the strong longitudinal component of the electric field in the focus of a sharply focused radially polarized beam. Radially polarized beams can also be used for particle guiding or trapping,<sup>3</sup> probing the orientation of single molecules,<sup>4</sup> optical tweezing,<sup>5</sup> or

beam guiding in metallic waveguides,<sup>6</sup> where the radial polarization shows low losses.

Radially, or equivalently, azimuthally, polarized light has been obtained by several methods. Two linearly polarized laser beams have been combined interferometrically, requiring subwavelength stable alignment and a high degree of coherence.<sup>7</sup> Interferometric stability is also required when radially polarized light is generated by intracavity coherent summation of two orthogonally polarized TEM<sub>01</sub> modes, by means of a birefringent beam displacer and a discontinuous phase element.<sup>8</sup> Space-variant subwavelength metal stripe gratings,<sup>9</sup> dielectric subwavelength gratings,<sup>10</sup> and a space-variant inhomogeneous medium<sup>11</sup> have been used to convert circularly (or linearly) polarized light into radial polarization. Besides the fact that these elements are used extracavity, their transmission efficiency is limited. Alternatively, radially polarized light can be excited when a polarization-selective element, exhibiting high losses for the tangential polarization and minimum losses for radially polarized radiation, is directly incorporated in a laser cavity. Radial polarization was produced with a conical Brewster window in a laser resonator.<sup>12,13</sup> A polarization-selective mirror based on a metallic diffraction grating was incorporated in a high-power CO<sub>2</sub> laser cavity.<sup>14</sup> The polarization selection is based on diffraction at a corrugated grating etched in the top of the metallic mirror. Polarization-selective mirrors based on a resonant coupling effect were used to generate radial polarization in Nd:YAG lasers.<sup>15</sup>

## 2. Giant Reflection to Zero Order

Here we present the development of a new polarization-selective laser mirror. A general demand

T. Moser and J. Balmer are with Institute of Applied Physics, University of Bern, Sidlerstrasse 5, CH-3012 Bern, Switzerland. D. Delbeke is with Department PIH, Hogeschool West-Vlaanderen, Graaf Karel de Goedelaan 5, B-8500 Kortrijk, Belgium. P. Muys is with Lambda Research Optics Europe, Tulpenstraat, 2, B-9810 Eke-Nazareth, Belgium. S. Verstuyft and R. Baets are with Ghent University-IMEC, Department Information Technology (INTEC), St. Pietersnieuwstraat, 41, B-9000 Ghent, Belgium.

Received 7 July 2006; revised 28 August 2006; accepted 29 August 2006; posted 29 August 2006 (Doc. ID 72676).

0003-6935/06/338517-06\$15.00/0

© 2006 Optical Society of America

on such elements used as laser cavity mirrors are low optical losses for the desired polarization. For a laser end mirror a reflectivity close to 100% is needed in order to guarantee efficient laser performance. In the development of the GIRO mirror (Giant Reflection to Zero Order)<sup>16</sup> great importance was attached on achieving high polarization selectivity and low losses for the desired polarization in order to use the element in a laser resonator. The first generation of radially polarized light in a CO<sub>2</sub> laser by means of GIRO is presented in this paper.

#### A. Design

The GIRO grating is a simple binary dielectric diffraction grating with adequately chosen period  $\Lambda$ , grating depth  $h$ , and filling factor  $f$  in order to achieve high polarization-selective reflection with a high reflectivity for the TM polarization at the same time. The parameters are sketched in Fig. 4. The working principle of the GIRO grating is based on the interference of two propagating modes in the grating region. For both polarizations (TE, TM) a pair of propagating modes in the grating region is excited with different effective indices. Due to this fact, a different reflection for TE and TM can be achieved. For TM the following effect takes place. At the ridges of the grating the two TM modes (which are the only excited modes) interfere destructively, and no coupling of optical power to the zero-order transmission will occur. In the grooves of the grating the two modes interfere constructively, maximizing the coupling to the zero-order reflection. For TE polarization the constructive interference occurs at the ridges, and the TE propagation modes interfere destructively in the grooves. This results in a high transmission and low reflection for TE polarization. A more detailed study of the GIRO principle is discussed elsewhere.<sup>17</sup> When the filling factor  $f$  (ratio of ridge width over period) of the grating is 0.5, this leads to the following approximate design rules for the GIRO grating:

$$\begin{aligned} f &\approx 0.5, \\ h/\lambda &\approx \frac{3/2}{(3n_1^2 + n_2^2)^{1/2} - n_2}, \\ \Lambda/\lambda &\approx \frac{2}{(n_1^2 - n_2^2)^{1/2}}, \end{aligned} \quad (1)$$

where  $\lambda$  is the wavelength of the incident light;  $n_1$  and  $n_2$  are the refractive indices of the ridges and the grooves of the grating, respectively. In order to design a GIRO for the use in a CO<sub>2</sub> laser, GaAs ( $n_2 = 3.27$ ) was chosen as the mirror substrate which is advantageous for its high refraction index. The design rules [Eq. (1)] are applied to the parameters  $\lambda = 10.6 \mu\text{m}$ ,  $f = 0.5$ ,  $n_1 = 3.27$ , and  $n_2 = 1$  from which the grating depth  $h$  and the grating period  $\Lambda$  result. Fine tuning of these parameters with the rigorous coupled-wave analysis (RCWA) results in a

**Table 1. GIRO Grating Designs Based on the Design Rules and on Calculations with RCWA<sup>a</sup>**

Method	$h$ ( $\mu\text{m}$ )	$\Lambda$ ( $\mu\text{m}$ )	$f$	$R_0^{\text{TM}}$	$R_0^{\text{TE}}$
Design Rules	3.34	6.797	0.5	98.6%	1.7%
RCWA	3.424	6.72	0.5	99.3%	6%

<sup>a</sup> $f = 0.5$ ,  $n_1 = 3.27$ ,  $n_2 = 1$ ,  $\lambda = 10.6 \mu\text{m}$ .

high zero-order TM reflection ( $>99\%$ ) in combination with a very low TE reflection to the zero order ( $<1\%$ ). The grating parameters obtained with the design rules [Eq. (1)] and the RCWA are summarized in Table 1. A reflectivity of nearly 100% for the TM polarization is possible with precisely controlled grating parameters. Figure 1 shows the diffraction efficiency based on the RCWA of a GIRO grating as a function of a varying grating depth  $h$  and grating period  $\Lambda$ . The third parameter is the lasing wavelength.

The GIRO grating does only show a high zero-order TM reflectivity when the light is incident from the high-refractive-index material as sketched in

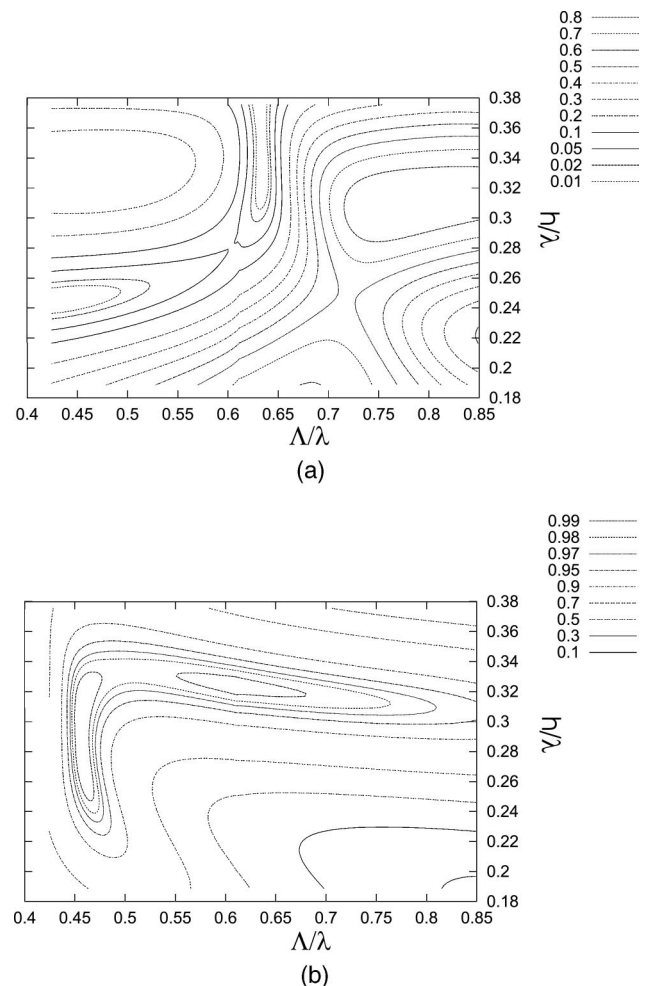


**Fig. 1. Simulation of the zero-order (a) TE reflectivity and (b) TM reflectivity over a large  $h$  and  $\Lambda$  range (normal incidence,  $f = 0.5$ ,  $n_1 = 3.27$ ,  $n_2 = 1$ ).**

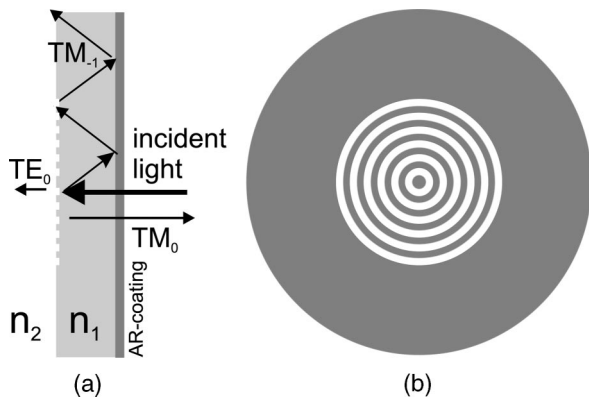


Fig. 2. Conceptual sketch of the radial polarizer based on a GIRO grating (a) cross section; (b) top view.

Fig. 2. The incident and reflected light hence propagate through the substrate. An antireflection (AR) coating prevents reflections at the high-contrast index interface (air/GaAs). This avoids the creation of etalon effects and thus guarantees a high TM reflectivity, independent of the thickness of the wafer. TE-polarized light incident on the GIRO grating is predominantly transmitted and only marginally reflected. The higher diffraction orders are totally internally reflected at the high-contrast index interface, irrespective of the presence of an AR coating. The wafer thickness can be chosen as thick to prevent backreflections on the grating, which could lead to high TE reflection due to constructive interference.

The design of the GIRO grating can be directly translated toward other high-refractive-index materials. The grating shows a low aspect ratio and can be defined in high-refractive-index materials such as InP, GaAs, and ZnSe with a reactive ion-etching processing scheme. These assets are convenient for use in high-power laser systems, where extremely high efficiencies are required to reduce costs, in combination with easy and cheap fabrication techniques to cope with the limited lifetime of optics used in damaging environments. A GIRO comprising a linear grating introduced as the end mirror in a laser reso-

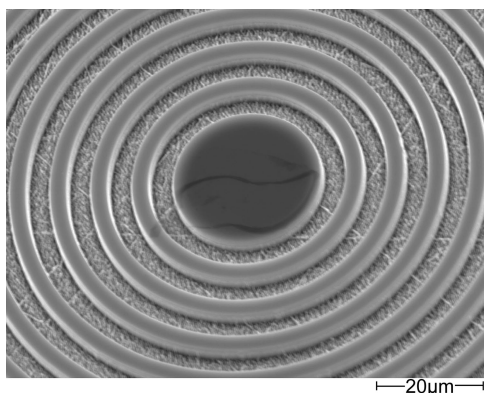


Fig. 3. SEM picture of a radial GIRO grating etched in a 3 mm thick GaAs wafer.

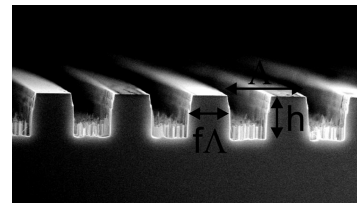


Fig. 4. SEM picture of a cut of a realized radial GIRO grating.

nator will result in a high reflection for the TM polarization. Consequently, a GIRO with a circular grating used as the end mirror in the laser cavity will result in a high reflection for the radially polarized modes.

## B. Fabrication and Characterization

A circular GIRO grating was fabricated in undoped GaAs to serve as the end mirror for a high-power CO<sub>2</sub> laser cavity. Photolithographic illumination ( $\lambda = 310$  nm) of a chromium mask was used to define the grating in photoresist (AZ5214) spun on the GaAs wafer. After development of the resist in a diluted solution of potassium hydroxide and a postbake, the resist pattern was transferred into the semiconductor using an ICP (inductive coupled plasma) reactive ion-etching system. The latter uses a SiCl<sub>4</sub>/Ar gas mixture at a pressure of 16 mTorr, an RF power of 150 W, and ICP power of 50 W. The ICP process is optimized to produce steep sidewalls (binary gratings with crenellated shape) and etches at a rate of 300 nm/min. The photoresist on top of the GaAs grating is removed with acetone. Since the GIRO is scheduled to serve as the end mirror in high-power CO<sub>2</sub> lasers, the mirror has to withstand the high laser power passing through it. Additionally the high pressure differential between the gas gain medium in CO<sub>2</sub> lasers (usually around 100 mbar) and atmosphere leads to a significant force on the GIRO. This force can induce bulging of the wafer. Also, to prevent constructive interference of the TE reflection to the higher orders (see above), the etching process of the grating was optimized for a wafer with a thickness of 3 mm. Figure 3 shows a picture of the fabricated grating taken with a scanning electron microscope (SEM) etched in a 3 mm thick GaAs substrate. Steep sidewalls were achieved, but not a perfectly smooth bottom. This could have its origin in defects caused during the polishing of the substrate. The control of the grating parameters is critical on the final reflectivity behavior of the GIRO. Figure 1 shows that the grating depth influences the TM reflectivity drastically, while

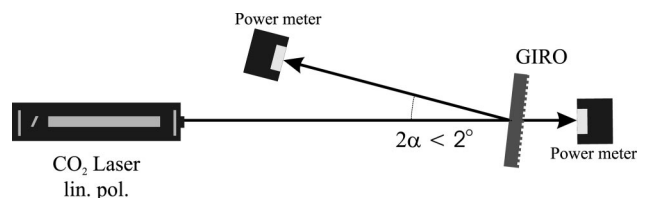


Fig. 5. Reflection and transmission measurement of the GIRO.



**Table 2. Comparison of the Simulated Parameters and the Fabricated Design at the Edge of the Grating<sup>a</sup>**

Realized GIRO	Simulation (edge)	Measurement (edge)
$R_0^{\text{TM}}$	93.5%	94%
$T_0^{\text{TM}}$	2.2%	1.0%
$R_0^{\text{TE}}$	14.9%	6%
$T_0^{\text{TE}}$	81.0%	82.0%

<sup>a</sup> $\lambda = 10.6 \mu\text{m}$ ,  $h = 3.7 \mu\text{m}$ ,  $\Lambda = 6.7 \mu\text{m}$ ,  $f = 0.47$ .

the grating period has more influence on the TE reflection. The filling factor highly affects the TE reflection, which is not very critical in the case of our final application as laser end mirror. In order to determine experimentally the realized grating parameters after etching, the sample was cleaved orthogonal to the grating lines, and the obtained cross section was then analyzed in a SEM (Fig. 4). The SEM characterization revealed a higher etching depth at the edge of the grating compared to the center, which leads to a nonuniform reflection behavior over the GIRO surface. A possible reason for this when thick wafers are used is not clear yet. Temperature, gas flow, and material quality are some possible factors. In the following, we distinguish between two positions on the grating: edge and center. The grating parameters obtained from the SEM analysis are the following: period  $\Lambda = 6.72 \mu\text{m}$ , grating depth edge  $h = 3.7 \mu\text{m}$ , grating depth center  $h = 3.3 \mu\text{m}$ , and filling factor  $f = 0.47$ . The accuracy of measuring the grating depth is found to be around  $\pm 50 \text{ nm}$  and for the filling factor  $\pm 0.01$ . The determined grating parameters were taken into the simulation in order to compare the realized grating with the optimized values based on the RCWA and the values obtained experimentally.

### C. TM/TE Reflectivity

The parameters of the grating such as period, groove depth, and filling factor are critical on the reflection behavior of the GIRO (Fig. 1). In order to measure the reflectivity and transmission for the two polarization states, the mirror was characterized in the setup shown in Fig. 5. The angle of inclination on the GIRO was kept small ( $\alpha < 1^\circ$ ) such as to minimize the deviation from results obtained at normal incidence. This is justified since, at an incident angle of  $1^\circ$ , the deviation for the TE/TM reflection is smaller than 0.5%/1.5%. The incident  $\text{CO}_2$  laser beam is linearly polarized, controlled by a Brewster plate in the res-

onator. The linear polarization was measured to be better than 100:1. To characterize the local reflection of the circular grating (with a diameter of 1 in.), the incident beam has to be relatively small in order to minimize the effect of the circular grating lines. Additionally the measurement was only performed at the edge of the grating. The incident beam has a diameter of 2.5 mm. The reflected and transmitted power was measured for both TE and TM polarization. In Table 2 the reflection and transmission parameters to the zero order are listed. The transmission for the undesired TE polarization is found to be over 80%, whereas for the TM polarization a high reflectivity to the zero order is present. Due to the high etching depth of  $3.7 \mu\text{m}$ , only 94% of reflectivity was achieved. The depth in the center of the grating will turn out to be more precise. The simulation as well as the reflectivity measurement are based on experimentally gained data. Therefore the deviation of the determined reflectivities in Table 2 is about  $\pm 2\%$  in both cases. As mentioned above, the filling factor highly affects the reflection to the zero order for the TE polarization. This explains the deviation in Table 2, as the filling factor is difficult to measure more accurately than  $\pm 0.01$  out of the not yet perfectly rectangular shape (Fig. 4). Nevertheless, a good agreement of the simulation based on the measured grating parameters and the experimentally determined reflectivities is shown.

### 3. Generation of Radial Polarization

The aim of the development was to generate radial polarization by means of a GIRO. In order to achieve only the radial polarization to oscillate, a distinctive difference in reflectivity for the radial and the tangential polarization at the high reflective laser mirror is needed. A laser mode with radial polarization will oscillate in the case that its lasing threshold and overall losses are lowest for this mode compared to the tangential analogy. The very low reflectivity for the TE polarization is not really needed as the lasing threshold will be much higher for the undesired state of polarization. Nevertheless, it can be an advantage in working with high gain lasers to still get a beam with a high polarization purity. For the generation of radial polarization, a sealed off  $\text{CO}_2$  laser tube was used as the gain medium. In order to have no additional polarization-selective element in the resonator, the tube is sealed with plano/plano AR-coated windows instead of the often-used Brewster windows. A

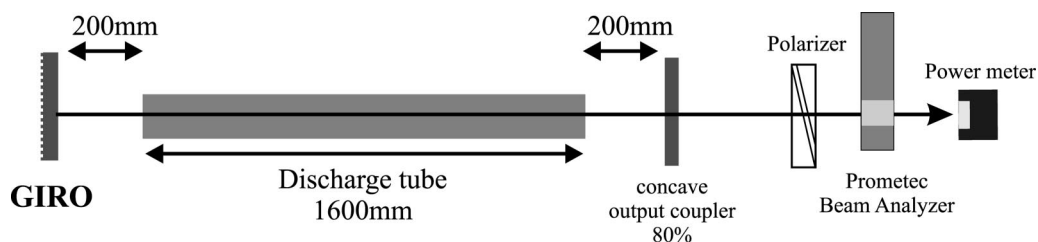


Fig. 6.  $\text{CO}_2$  laser setup used to generate radial polarization.

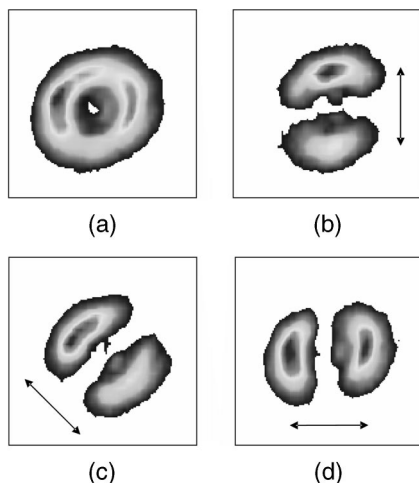


Fig. 7. Intensity distribution of the radially polarized  $\text{CO}_2$  laser beam: (a) without polarizer, and through a polarizer oriented (b) vertically, (c) at  $45^\circ$ , and (d) horizontally.

concave output coupling mirror with a reflectivity of 80% and the GIRO used as the end mirror completed the resonator (Fig. 6). The output beam was characterized with a setup consisting of a polarizer with two GaAs Brewster plates, a Prometec beam analyzer system, and a powermeter. For the first time to our knowledge, intracavity generation of radial polarization in a  $\text{CO}_2$  laser by means of a GIRO was shown. Figure 7(a) shows the fundamental doughnut mode emitted by the laser. The polarization is purely radial, which is proved by measuring the beam after passing the polarizer oriented in different directions [Figs. 7(b)–7(d)]. The bowtie-like beam profile is oriented in the same direction as the polarizer, which proves the electric field of the generated laser beam to be in the radial direction throughout the beam.

The polarization purity was determined by the following method. The laser power was measured after transmittance through a polarizer oriented at different angles. If the through power was independent of the direction of the polarizer and was always half of the incident power, this proved a radially symmetric polarization distribution. In the experiment, variations of smaller than 5% were found.

To prove radial polarization, the intensity distribution after the polarizer had to be taken into account as well. The intensity distribution of the lowest-order purely radially polarized laser beam after a polarizer is equal to a  $\text{TEM}_{01}$  mode pattern. Therefore the degree of polarization was determined by calculating the angular correlation of the intensity distribution after a polarizer, once in the horizontal and once in the vertical direction. By this, the radially symmetric intensity distribution as well as the correlation to radial polarization was taken into account. With this method, the radial polarization purity was found to be higher than 90%. This implies that 90% of the laser power would be transmitted through a radial polarizer.

Figure 8 shows the cross section of the doughnut mode in the horizontal direction. The experimentally

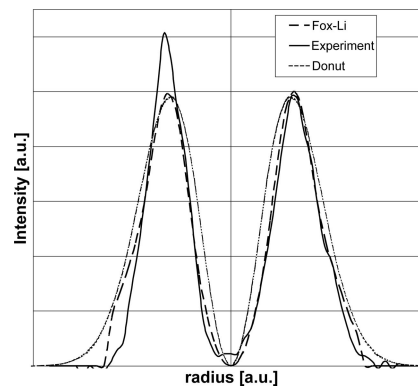


Fig. 8. Horizontal cross section of the radially polarized doughnut mode. Comparison of the experimental data, the theoretical  $\text{TEM}_{01}$  mode, and the Fox–Li simulation taking the diffraction losses into account.

determined mode shape shows steeper edges than the theoretical  $\text{TEM}_{01}$  intensity distribution. To explain the difference, further simulations have been carried out. With the Fox–Li algorithm<sup>18</sup> the oscillating mode is calculated taking the diffraction losses at the aperture in the resonator into account. A comparison with the experimental data shows an improved agreement. The diffraction losses are due to the resonator design with a low Fresnel number. We note that the GIRO behaves as a plane mirror. The GIRO can work as a curved mirror by applying an appropriate radius of curvature to the incident plane that induces a lens. By this the resonator can be driven in a stable range for the doughnut mode. Figure 9 shows the output power of the  $\text{CO}_2$  laser achieved with a standard high-reflecting mirror and the GIRO used as end mirror. Radially polarized laser beams with an optical power up to 45 W were achieved, limited by the available laser system. Figure 9 shows a decreased slope efficiency for the GIRO configuration. There are different reasons. First, the nonperfect reflection at the GIRO causes higher roundtrip losses. The simulation gives a reflectivity of about 96% for the TM polarization

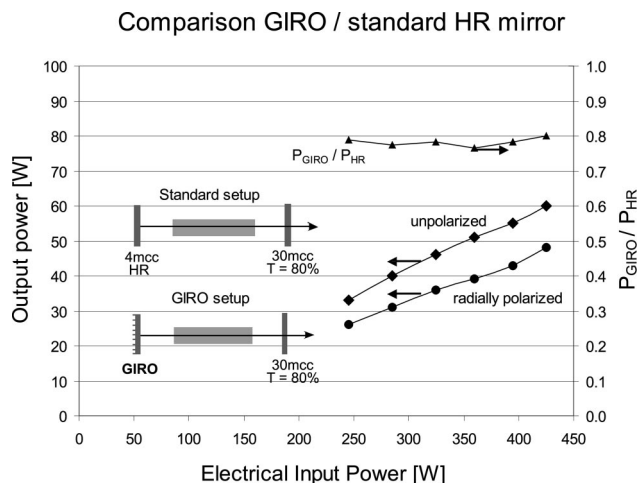


Fig. 9. Comparison of the output power of the resonator with a standard HR mirror and with the GIRO.

**Table 3. Simulated Parameters Based on the Measured Parameters at the Center of the Grating<sup>a</sup>**

Realized GIRO	$R_0^{\text{TM}}$	$R_0^{\text{TE}}$
Simulation (center)	95.8%	1.8%

<sup>a</sup> $\lambda = 10.6 \mu\text{m}$ ,  $h = 3.3 \mu\text{m}$ ,  $\Lambda = 6.72 \mu\text{m}$ ,  $f = 0.47$ .

(Table 3). Second, the doughnut mode shows a singularity in the center, which gives a lower overlap of the gain and the laser mode cross sections. Additionally, the resonator is working at the stability limit whereby high diffraction losses occur. This is clearly visible in the cross section of the output laser beam (Fig. 8).

#### 4. Conclusion

We conclude that with the use of a simple binary diffraction grating, a laser can excite radially polarized light. An advantage of the presented method is its simplicity. No additional element or setup is needed; the laser resonator end mirror is replaced by an optimized GIRO. Intracavity generation of radial polarization with high efficiency and simultaneously high polarization purity (90%) were shown in this paper. Good agreement of the simulation and the experimental verification has been shown. This implies that with an improved control of the etching process, a GIRO with a reflectivity for the TM polarization near 100% can be achieved. The method is expected to be suitable for high-power application. The mirror is a monolithic element made out of GaAs, a well known material in high-power applications. Laser mirrors with optimized grating depth and filling factor are now being processed to be used in a kW-laser system in order to generate high-power radially polarized CO<sub>2</sub> laser beams.

The authors acknowledge Bart Dhoedt and Stefan Goeman for exploring research on the GIRO grating, and Liesbet Van Landschoot and Eva Krähenbühl for technical support. Danaë Delbeke thanks the IWT (Institute for the Promotion of Innovation by Science and Technology in Flanders) for financial support.

#### References

1. V. G. Niziev and A. V. Nesterov, "Influence of beam polarization on laser cutting efficiency," *J. Phys. D: Appl. Phys.* **32**, 1455–1461 (1999).
2. W. D. Kimura, G. H. Kim, R. D. Romea, L. C. Steinhauer, I. V. Pogorelsky, K. P. Kusche, R. C. Fernow, X. Wang, and Y. Liu, "Laser acceleration of relativistic electrons using the inverse Cherenkov effect," *Phys. Rev. Lett.* **74**, 546–549 (1995).
3. T. Kuga, Y. Torii, N. Shiokawa, T. Hirano, Y. Shimizu, and H. Sasada, "Novel optical trap of atoms with a doughnut beam," *Phys. Rev. Lett.* **78**, 4713–4716 (1997).
4. L. Novotny, M. R. Beversluis, K. S. Youngworth, and T. G. Brown, "Longitudinal field modes probed by single molecules," *Phys. Rev. Lett.* **86**, 5251–5254 (2001).
5. Q. Zahn, "Trapping metallic Rayleigh particles with radial polarization," *Opt. Express* **12**, 3377–3382 (2004).
6. M. E. Marhic and E. Garmire, "Low-order TE<sub>0q</sub> operation of a CO<sub>2</sub> laser for transmission through circular metallic waveguides," *Appl. Phys. Lett.* **38**, 743–745 (1981).
7. S. C. Tidwell, D. H. Ford, and W. D. Kimura, "Generating radially polarized beams interferometrically," *Appl. Opt.* **29**, 2234–2239 (1990).
8. R. Oron, S. Blit, N. Davidson, A. A. Friesem, Z. Bomzon, and E. Hasman, "The formation of laser beams with pure azimuthal or radial polarization," *Appl. Phys. Lett.* **77**, 3322–3324 (2000).
9. Z. Bomzon, V. Kleiner, and E. Hasman, "Formation of radially and azimuthally polarized light using space-variant subwavelength metal stripe gratings," *Appl. Phys. Lett.* **79**, 1587–1589 (2001).
10. Z. Bomzon, G. Biener, V. Kleiner, and E. Hasman, "Radially and azimuthally polarized beams generated by space-variant dielectric subwavelength gratings," *Opt. Lett.* **27**, 285–287 (2002).
11. Ch. Tsai, U. Levy, L. Pang, and Y. Fainman, "Form-birefringent space variant inhomogeneous medium element for shaping point-spread functions," *Appl. Opt.* **45**, 1777–1783 (2006).
12. Y. Mushiake, K. Matsumura, and N. Nakajima, "Generation of radially polarized optical beam mode by laser oscillation," *Proc. IEEE* **60**, 1107–1109 (1972).
13. Y. Kozawa and S. Sato, "Generation of a radially polarized laser beam by use of a conical Brewster prism," *Opt. Lett.* **30**, 3063–3065 (2005).
14. A. V. Nesterov, V. G. Niziev, and V. P. Yakunin, "Generation of high-power radially polarized beam," *J. Phys. D: Appl. Phys.* **32**, 2871–2875 (1999).
15. T. Moser, H. Glur, V. Romano, M. A. Ahmed, F. Pigeon, O. Parriaux, and Th. Graf, "Polarization-selective grating mirrors used in the generation of radial polarization," *Appl. Phys. B* **80**, 707–713 (2005).
16. R. Baets, B. Demeulenaere, B. Dhoedt, and S. Goeman, "Optical system with a dielectric subwavelength structure having high reflectivity and polarization selectivity," U.S. Patent 6191890 B1 (20 February 2001).
17. D. Delbeke, R. Baets, and P. Muys, "Polarization selective beamsplitter based on a highly efficient simple binary diffraction grating," *Appl. Opt.* **43**, 6157–6165 (2004).
18. E. Sziklas and A. Siegman, "Mode calculations in unstable resonators with flowing saturable gain. 2: Fast Fourier transform method," *Appl. Opt.* **14**, 1874–1889 (1975).